

LGS alternative wave-front sensing: Projected Pupil Plane Pattern (PPPP)

Huizhe Yang^a, Alastair Basden^a, David Buscher^b, Francisco Javier De Cos Juez^c, Aglae Kellerer^d, Tim Morris^a, Richard Myers^a, Eddy Younger^a, and Nazim Bharmal^a

^aCentre for Advanced Instrumentation, Department of Physics, Durham University, South Road, Durham DH1 3LE, UK

^bCavendish Laboratory, JJ Thomson Avenue, Cambridge CB3 0HE, UK

^cDepartment of Applied Mathematical Modelization, University of Oviedo, Oviedo, Spain

^dEuropean Southern Observatory, Garching bei Munchen, Germany

ABSTRACT

For the next generation of extremely large telescopes with the primary mirrors over 30 m in diameter, focal anisoplanatism renders single laser guide star AO useless. The laser tomography AO (LTAO) technique demonstrates an effective approach to reduce focal anisoplanatism, although it requires multiple LGSs & WFSs, and complex tomographic reconstruction. Here we propose a novel LGS alternative configuration with the corresponding wavefront sensing and reconstruction method, termed Projected Pupil Plane Pattern (PPPP). A key advantage of this method is that a single collimated beam is launched from the telescope primary mirror, and the wavefront sensed on the uplink path, which will not suffer from the effects of focal anisoplanatism. In addition, the power density of the laser beam is significantly reduced compared to a focused LGS, which decreases aircraft and satellite safety hazards. A laboratory experiment for PPPP has been setup to anchor the PPPP concept and compare against a Shack-Hartmann WFS.

Keywords: Adaptive Optics, LGS, PPPP, Laboratory experiment

1. INTRODUCTION

The Pupil Plane Projected Pattern (PPPP) technique was developed by Buscher et al¹ as a concept in 2002 to overcome the then-unsolved problem of focal anisoplanatism for giant telescopes – Extremely Large Telescopes – when using laser beacons (Laser Guide Stars, LGS) as sources for WFSs. The origin of focal anisoplanatism² known also as the cone effect is from the finite altitude of the LGSs generated at either 5-20 km (Rayleigh) or 90 km (Sodium) from a ground-projected laser. The LGS is intended to be a compact source which emits light downwards to be an alternative to light from a star (referred to as a Natural Guide Star, NGS). Therefore, the volume of the atmosphere probed by a LGS is a cone, while the corresponding volume probed by a NGS is cylinder. For a 4-m-class telescope, the mismatch between a Sodium LGS cone centred above the telescope and the cylinder probed by light from a NGS results in relatively little error in the measured wavefront (note that measurements from a LGS are always corrupted by high-order aberrations and so measurement error must always be augmented by those from a LGS than a NGS). For larger telescope diameters, such as the proposed next-generation optical ground-based Extremely Large Telescopes (ELTs) with primary mirror diameters of over 30 m, the wavefront error caused by focus anisoplanatism can reach ~155 nm rms (root mean square) on the 10-m Keck telescope, Hawaii, US, according to Bouchez³ and over 300 nm for ELTs⁴. The common approach to solve the focal anisoplanatism now is to use Laser tomography AO (LTAO), where multiple LGSs and WFSs are required to estimate the 3D turbulence. LTAO introduces enormous complexity and expense from using multiple LGSs and tomographic reconstruction, and the complexity and expense scale with the number of LGSs used. Additionally for Sodium-based LGS, due to the mesospheric sodium density distribution in altitude, these LGSs

Further author information: (Send correspondence to Huizhe Yang)

Huizhe Yang: E-mail: huizhe.yang@durham.ac.uk, Telephone: 00447421306728

produce sources elongated in the laser projection direction. The elongation consequence is the WFS images are non-homogeneous with increasing perspective lengthening of the beacon when it is viewed from a non-centred location. As this off-axis lengthening always occurs, this produces an additional measurement error within the WFS. Therefore the use of multiple LGSs with elongated beacons and the associated tomography algorithms are complicated and expensive, and can not provide complete measurements of the wavefront. Thus far, their use has been limited to near-infrared observations but not used effectively at shorter wavelengths.

In contrast PPPP is designed to overcome the issues with using the multiple-LGS-and-tomography solution. First, for PPPP the laser beam is projected as an afocal beam: formally, this means the guide star concept has no meaning. Therefore, WFSs as traditionally understood are not used and instead a beam profile re-imaging camera is used. Since there is no requirement to focus the beam in the atmosphere, and by expanding the beam to equal the telescope primary diameter, the volume of atmosphere probed by the PPPP beam then becomes equivalent to that illuminated by a NGS, PPPP is free of cone effect.

In this paper we demonstrate the PPPP concept by a laboratory experiment. In Section 2 we briefly introduce the PPPP theory and simulation modeling. In section 3 we describe the PPPP laboratory experiment and show the bench results. In section 4 we draw our conclusions.

2. PPPP THEORY AND SIMULATION PROCESS

Detailed description and analysis regarding PPPP theory and simulation modeling have been presented in Huizhe Yang.⁵ Here we only briefly recall the PPPP theory and simulation process. PPPP is based on the transport-of-intensity equation (TIE),

$$k\partial_z I = -\nabla \cdot (I\nabla\phi), \quad (1)$$

which can be approximated as,

$$k\frac{I_2 - I_1}{h_2 - h_1} = -\nabla \cdot (I_0\nabla\phi) = -\nabla I_0 \cdot \nabla\phi - I_0\nabla^2\phi, \quad (2)$$

where I_0 , I_1 and I_2 are the intensity patterns at the propagation distances 0, h_1 and h_2 respectively. Given I_0 , I_1 and I_2 , we can retrieve the phase ϕ except piston according to equation (2). As for PPPP, the basic setup is illustrated in Fig.1. A laser beam is expanded to fill the pupil of the telescope and propagates as a collimated beam upward through the atmosphere. When the laser pulse reaches an altitude of h_1 , a snapshot of the Rayleigh backscattered radiation is taken with a camera conjugate at h_1 , which will show a disk of illumination corresponding to the telescope pupil (i.e. I_1). When the laser pulse reaches an altitude of h_2 , a second snapshot is taken with a camera conjugate at h_2 . With the obtained I_1 and I_2 we can retrieve the turbulence phase ϕ according to equation (2). To control the propagation distance, a pulsed laser and mechanical shutter are required. Specifically when the pulsed laser reaches h_1 and scattered back, the shutter is opened at time point $(2 \times h_1)/c$. When the laser beam continues propagating to $h_1 + \Delta h_1$ and scattered back, the shutter is closed at time point $(2 \times h_1 + 2 \times \Delta h_1)/c$. Δh_1 is the range gate depth for h_1 . Similarly for h_2 , we open the shutter at $(2 \times h_2)/c$ and close it at $(2 \times h_2 + 2 \times \Delta h_2)/c$ for h_2 . This mechanical shutter is controlled in this manner for each laser pulse.

According to the PPPP theory, PPPP simulation modeling is divided into three steps: firstly to propagate a collimated beam upwards from the telescope pupil plane to two altitudes - termed upward propagation; then to reimage the Rayleigh backscattered intensity patterns at those altitudes through the same telescope by cameras conjugate at the corresponding heights - termed return path; finally to retrieve the distorted phase using the subtraction of the images from these cameras - termed reconstruction. The images have to be scaled to the same flux to satisfy the conservation of energy.

3. EXPERIMENTAL DESCRIPTION

3.1 Experimental setup

The laboratory setup for PPPP is shown in Fig.2. This setup includes propagating the laser beam to two different distances (i.e. the upward propagation) and re-imaging the back-scattered light from the scatter screen. In this

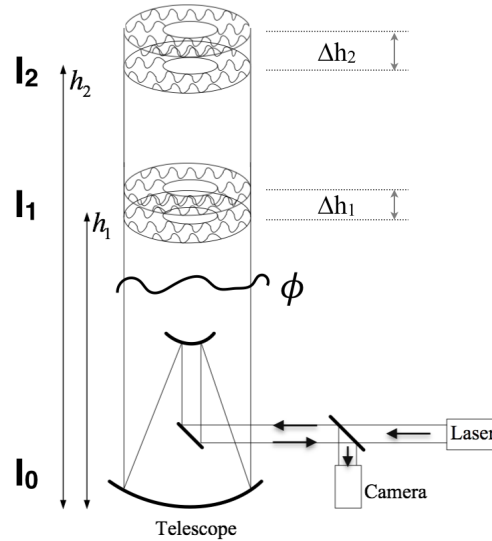


Figure 1. Schematic diagram of PPPP.

design the images of the back-scattered pattern for different propagation distance can be kept similar size and the signal for PPPP is the subtraction of these two images. The SH Arm is used to calibrate the DM and compare with PPPP. The parameters are listed in Table 1. The actual laboratory experiment is shown in Fig.3.

3.2 DM calibration

The DM used in this experiment is a 40-actuators Piezoelectric DM, with circular keystone deformable mirror actuator array (shown in Fig.4). This DM is ideal for correcting distortions that result from common sources of wavefront aberrations, such as astigmatism and coma, and include separate mechanisms to adjust for tip and tilt. However the problem with this DM is that the Hysteresis of Piezoceramic Material can reach 15% and even more. Thus it is of great importance to control the DM shape precisely. To achieve so, we use the SH WFS to build a closed-loop AO control and let the reference slope be some certain one associated with some certain DM shape. Thus within several iterations the measured slope will close in on the reference slope and in this way the DM shape can be controlled precisely the same as the reference one.

Zernike polynomials are used in the SH closed loop control as it is very handy for this DM to generate Zernike modes, from defocus (4-th Zernike mode) to 15-th Zernike mode. As any AO calibration process, individual Zernike mode are generated and the corresponding slopes are placed in a matrix, termed interaction matrix. The control matrix is then the pseudo-inversion of this interaction matrix. Given the control matrix, we can get the reconstructed 12 Zernike coefficients by multiplying this control matrix with the subtraction of the measured slope and the reference slope. The reference slope is obtained by setting the DM shape as any shape we want. Thus within several iterations we can control the DM shape precisely the same as the reference one. Fig.5 shows the relative slopes error variance with and without the AO closed loop control within 10 hours. We can see that with the closed loop AO control the slopes error variance stays almost the same within this 10 hours and this ensures the stability and precision of the DM shape.

3.3 PPPP pipeline

3.3.1 PPPP signal

As described in section 2, PPPP signal is the subtraction of intensity patterns at h_1 and h_2 , i.e. I_1 and I_2 respectively. Corresponding to the experiment, I_1 is the image when the mirror pair is in position 1 and I_2 is in

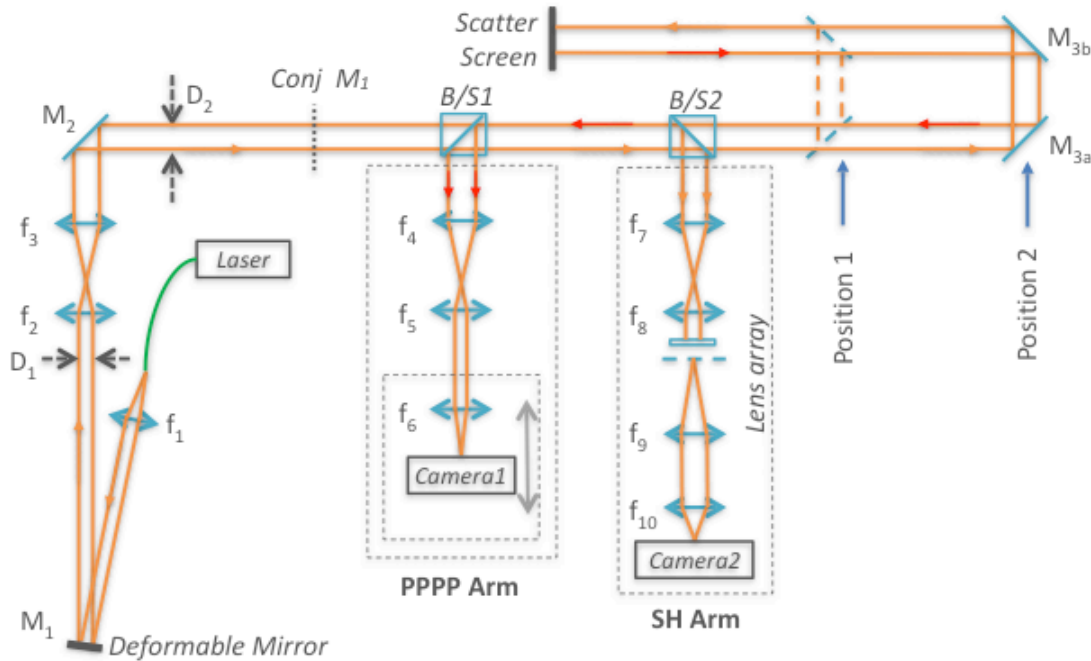


Figure 2. Optical layout of PPPP. A 633 nm laser beam is confined into a single mode fiber and the other end of the fiber is mounted on a pinhole, performing as a point source. After passing through the lens f_1 we get a collimated beam from the point source. The collimated beam then reaches the Deformable Mirror. Here the DM performs as an atmosphere simulator to generate random aberrations and the DM is conjugate to somewhere before the beam splitter 1. f_2 and f_3 are the optical relay to change the beam diameter from D_1 mm to D_2 mm. The beam transmits through B/S1 and then divided into two parts at B/S1. The first one (10% reflect light from B/S2) is for the SH WFS, and the second part (90% transmission light) propagates to the Scatter Screen (here a highly reflective piece of paper is used) via the mirror pair $M_{3a,b}$. The propagation distance can be changed by moving the mirror pair from position 1 to position 2. Then the scattered light from the Scatter Screen travels back through $M_{3a,b}$ and picked off by B/S1, into the PPPP Arm to re-image the back-scattered light from the Scatter Screen. The advantage of this design is that when moving $M_{3a,b}$ to change the propagation distance, we can simply get the corresponding images without changing the image size by moving f_6 and camera 1 together with fixed distance in between. f_4 and f_5 are another optical relay to decrease the beam size, and f_6 and camera 1 are used to get the image of the back-scattered pattern.

position 2. Images of I_1 and I_2 with flat DM (all actuators are set to 100 volts) are shown in top row of Fig.6 and the corresponding PPPP signal $I_2 - I_1$ is at the last column. As we can see, the images are very speckled because of the diffuse reflections of laser light acting on the fixed scatterer screen. In reality the atmospheric molecules moves very fast with time scale \sim several ns and the laser speckle will be averaged out. To simulate the atmospheric molecules moving, we simply place the scatterer screen on a rotating mini fan to get rid of the speckles (the corresponding images are shown in bottom row of Fig.6). Due to the optical static aberrations and diffraction effect, it is not possible to get exactly the same I_1 and I_2 . Thus $I_2 - I_1$ (the image at the right bottom in Fig.6) is initial reference PPPP signal and should be subtracted from the measured signal when other distortions are introduced from the DM.

3.3.2 PPPP calibration

There are two ways for PPPP calibration. One is to generate individual Zernike mode by the DM and get the corresponding PPPP signal ($I_2 - I_1$), placed in so-called measured interaction matrix. The other is to calculate a theoretical interaction matrix according to Yang^{5 & 6}. Then the control matrix is simply the pseudo-inversion of the interaction matrix, either the measured or theoretical one. In this paper we adopt the first option in order

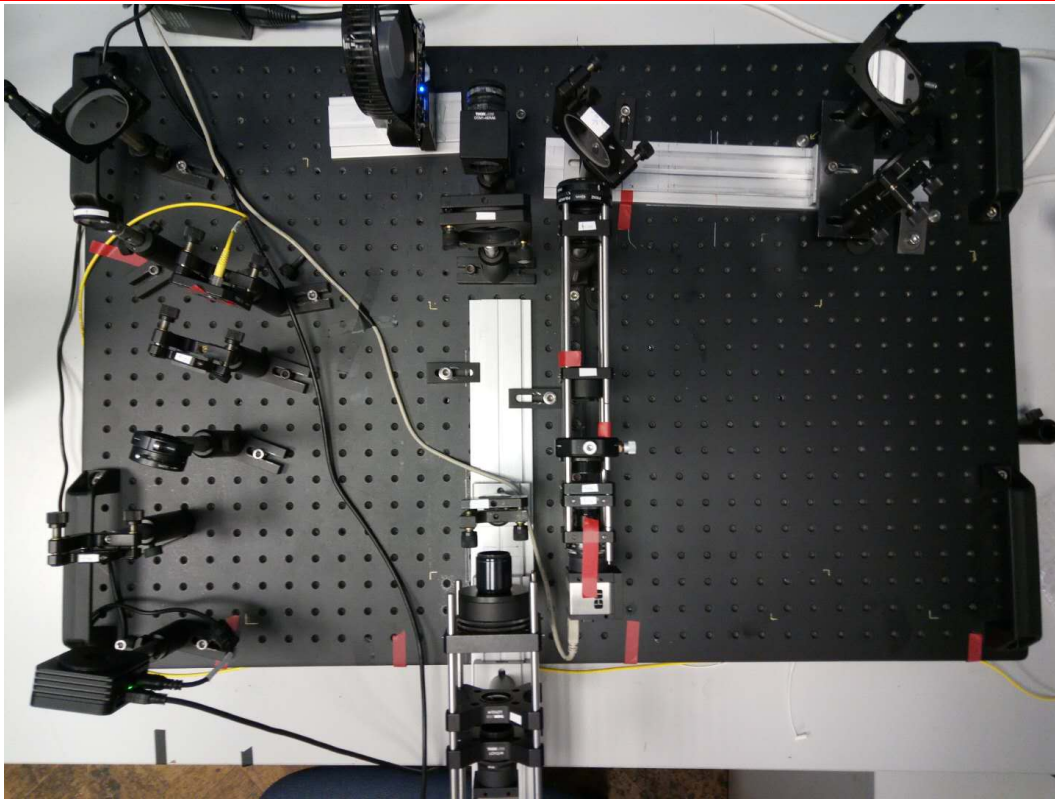


Figure 3. The laboratory experiment. In this figure the mirror pair is at Position 2.

Table 1. Parameters of PPPP experiment shown in Fig.2. The unit is mm. The lenslet is 10mm square with 500um pitch.

$D_1=12$	$D_2=18$	$z_1=600$	$z_2=900$	$\lambda = 633\text{nm}$
$f_1=50$	$f_2=100$	$f_3=150$	$f_4=150$	$f_5=75$
$f_6=100$	$f_7=100$	$f_8=25$	$f_9=30$	$f_{10}=16$
B/S1: 50:50 R:T		B/S2: 10:90 R:T		

to cancel out the static aberration from the optical system, especially the difference of the optical aberration between position 1 and position 2 when re-imaging the scattered pattern. It is worth to note that each Zernike mode is generated twice, with an equal positive and negative magnitude. Then the corresponding PPPP signal is the subtraction of the PPPP signal for positive and negative magnitude separately divided by two. The measured control matrix is shown in Fig.7.

3.3.3 Results

Given the measured control matrix, now we are able to reconstruct the optical distortions introduced by the DM. Specifically when a random aberration is generated by the DM, we measure the corresponding I_1 and I_2 and get the corresponding PPPP signal $I_2 - I_1$. Then multiplying the PPPP signal (subtraction of the measured PPPP signal and the reference PPPP signal when the DM is flat) with the control matrix, we can get the reconstructed 12 Zernike coefficients. Fig.8 shows the average relative error variance of the reconstructed Zernike coefficients from 50 random aberrations generated by the DM. The x-axis is the pixel number of the binned images and binning the images can reduce some high-order static optical aberrations from this bench experiment to increase decrease the measurement error. We can see that the PPPP error variance increases rapidly when the pixel

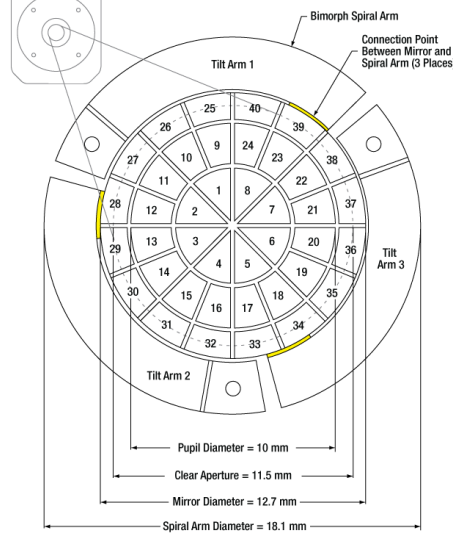


Figure 4. The circular keystone deformable mirror actuator array (Thorlab website).

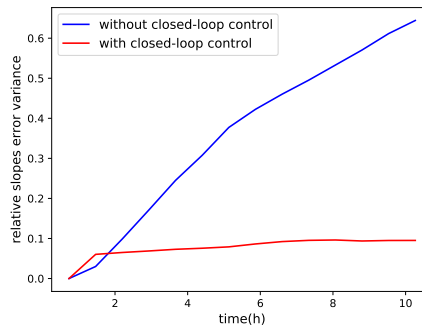


Figure 5. Relative slopes error variance with and without the AO closed loop control within 10 hours. The error variance is an average of DM shape from 4-th Zernike mode to 15-th Zernike mode.

number increases, and the minimum relative error variance is 0.26 when $N=8$ & 16. Thus we adopt the choice of $N=16$. The corresponding relative error variance for SH WFS is 0.12. As the propagation distance is controlled by moving the mirror pair manually, as well as moving the lens f_6 and camera 1, it is very time-consuming. Thus we collect 50 sets of I_1 and I_2 for these 50 random aberrations separately. To make sure the DM shape are remained the same while collecting I_1 and I_2 , we use the SH closed loop control as described in section 3.2.

The above results are based on the wavefront measurement, instead of a complete AO closed-loop system. To perform so, after the reconstructed Zernike coefficients are obtained for one random distortion introduced by the DM, we apply the reconstructed Zernike coefficients on the DM to correct the distortion. Then from the current DM shape we measure the PPPP signal and repeat the reconstruction. Within several iterations the DM should be approaching to the reference shape, where all the actuators are given a voltage of 100V (the range is 0 to 200V). So here we adopt an internal closed-loop AO control (with the DM performing as the turbulence simulator and wavefront corrector at the same time). One example of AO closed-loop control with both PPPP and SH WFS are shown in Fig.9. As can be seen the SH closed loop converges more quickly than PPPP, while they both can converge to similar level.

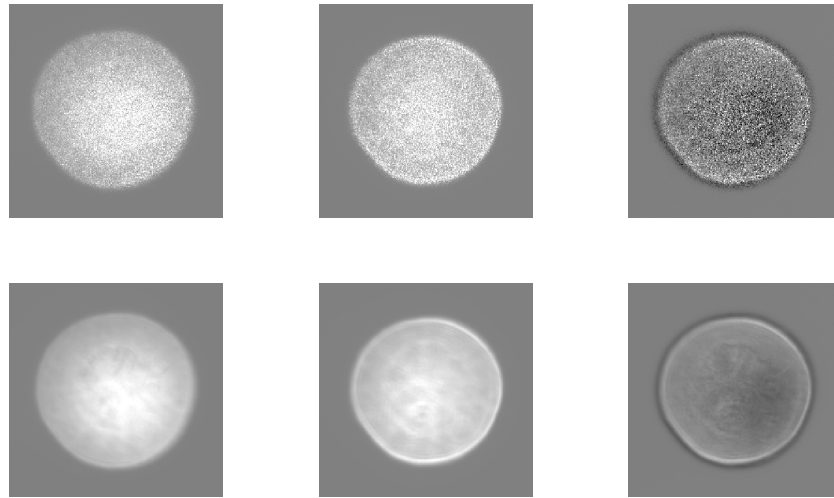


Figure 6. Images of backscattered patterns with flat DM. The top row is with fixed scatter screen and the bottom row is with scatter screen placed on a rotating mini fan. The left column is I_1 , the middle column is I_2 and the right column is I_2-I_1 . The images in first and second column have been scaled to the same flux to satisfy the conservation of energy and all the images are shown on a same scale.

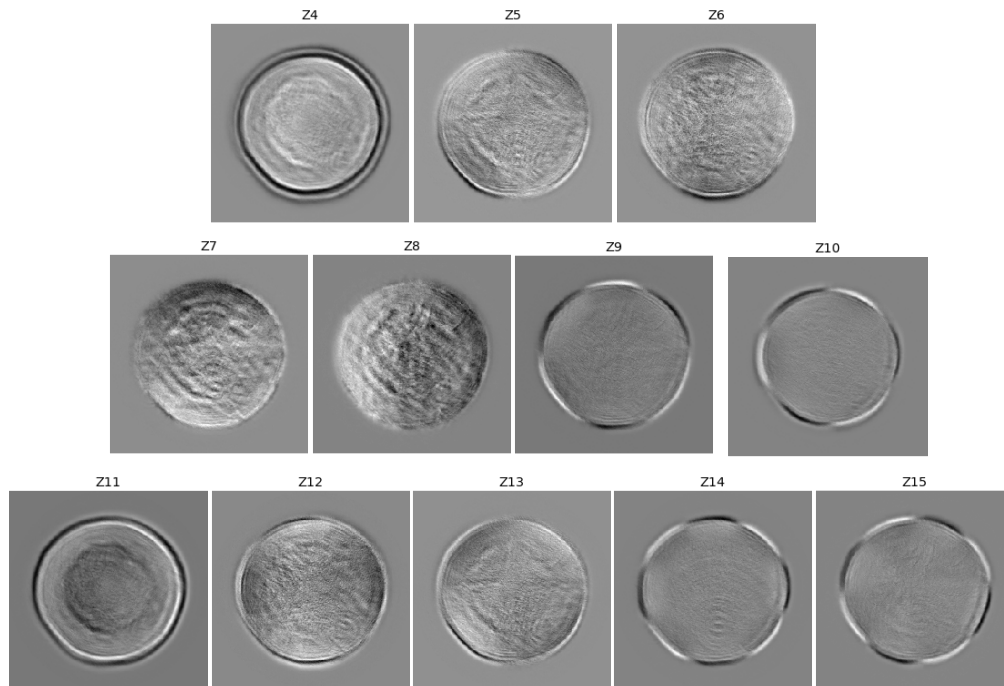


Figure 7. 2D display of the measured control matrix for each Zernike mode. For most modes the measured signal are consistent with the theoretical Zernike modes except coma (Z7 and Z8), which is due to the error when the DM generate the corresponding Zernike modes.

4. CONCLUSION

We have demonstrated a novel alternative LGS scheme – Projected Pupil Plane Pattern (PPPP) and its corresponding wavefront sensing and reconstruction method from a laboratory experiment. The laboratory experiment

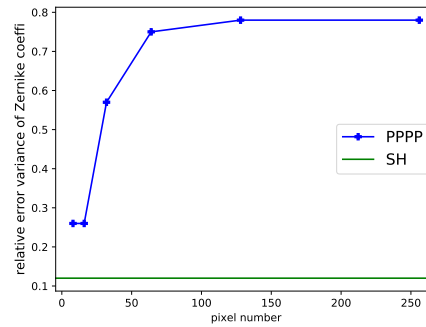


Figure 8. The error variance of the reconstructed Zernike coefficients divided by the variance of the input Zernike coefficients. It is an average result of 50 random aberrations. The x-axis is the pixel number of the binned image across the pupil and the original unbinned image is 256 by 256.

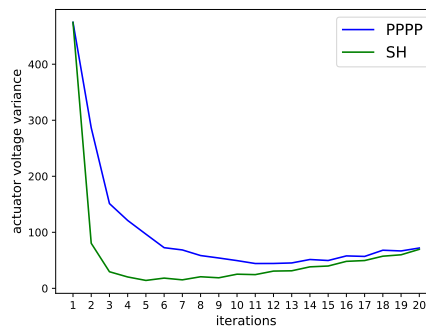


Figure 9. One example of AO closed-loop control with both PPPP and SH WFS. The y-axis is the actuator voltage variance (the unit is Volts²) and x-axis is the iterations.

includes laser propagation with changeable distance, re-imaging optical system for the scattered light, and a SH WFS for comparison. An advantage of this design is that the size of the images of the scattered pattern with different propagation distance can be kept similar, by simply moving the focus lens and PPPP camera together on a rail with fixed distance in between. We have used the SH to build a closed loop AO system to control the DM shape precisely without changing in time. We have build a measured control matrix from 12 Zernike modes generated by the DM. The reconstructed results have be shown to verify the PPPP concept. We have also performed a closed loop AO system with both PPPP and SH WFS, and these two provide similar residual error within 20 iterations.

ACKNOWLEDGMENTS

All authors acknowledge STFC funding ST/P000541/1. HY acknowledges CSC funding.

REFERENCES

- [1] Buscher, D. F., Love, G. D., and Myers, R. M., "Laser beacon wave-front sensing without focal anisoplanatism," *Optics Letters* **27**, 149–151 (2002).
- [2] Hardy, J., [*Adaptive Optics for Astronomical Telescopes*], Oxford University Press, Oxford (1988).
- [3] Bouchez, A., "Keck laser guide star adaptive optics: science verification results," *Proceedings of Advancements in Adaptive Optics* **5490**, 321–333 (2004).

- [4] Gavel, D. and Neyman, C., “Tomography codes comparison and validation,” *Keck Adaptive Optics Note 475* (2007).
- [5] Yang, H., Bharmal, N. A., and Myers, R. M., “Projected pupil plane pattern: an alternative lgs wavefront sensing technique,” *Monthly Notices of the Royal Astronomical Society* **477**(4), 4443–4453 (2018).
- [6] Gureyev, T. E. and Nugent, K. A., “Phase retrieval with the transport-of-intensity equation. ii. orthogonal series solution for nonuniform illumination,” *J. Opt. Soc. Am. A* **13**, 1670–1682 (Aug 1996).